European Review for Medical and Pharmacological Sciences 2020; 24: 2659-2666

MiR-26a inhibits myocardial cell apoptosis in rats with acute myocardial infarction through GSK-3β pathway

S. LU[1], Y. LU[2]

[1]Department of Emergency Medicine, First Affiliated Hospital of Jinzhou Medical University, Jinzhou, China
[2]Department of Emergency Medicine, Huludao Central Hospital, Huludao, China

Abstract. – OBJECTIVE: To study the influence of micro ribonucleic acid (miR)-26a on myocardial cell apoptosis in rats with acute myocardial infarction (AMI) through the glycogen synthase kinase 3 beta (GSK-3β) pathway.

MATERIALS AND METHODS: A total of 36 Sprague-Dawley rats were randomly divided into sham group (n=12), model group (n=12), and miR-26a mimics group (n=12). Only the heart was exposed, and normal saline was intraperitoneally injected postoperatively in sham group, and the model of AMI was prepared in model group. Besides, after modeling, miR-26a mimics were injected into the left ventricle in miR-26a mimics group. At 48 h after operation, sampling was performed. Then, the expressions of B-cell lymphoma 2 (Bcl-2) and Bcl-2 associated X protein (Bax), as well as the protein expression of phosphorylated GSK-3β (p-GSK-3β) were detected via immunohistochemistry and Western blotting, respectively. Moreover, the expression level of miR-26a was measured via quantitative polymerase chain reaction (qPCR), and cell apoptosis was evaluated using terminal deoxynucleotidyl transferase (TdT) dUTP nick-end labeling (TUNEL) assay.

RESULTS: Compared with those in sham group, the expression level of Bax was substantially raised, but that of Bcl-2 was notably lowered in model group and miR-26 mimics group ($p<0.05$), and miR-26 mimics group had a markedly lower expression level of Bax and a remarkably higher expression level of Bcl-2 than model group ($p<0.05$). According to Western blotting results, the protein expression level of p-GSK-3β in model and miR-26a mimics groups was considerably higher than that in sham group ($p<0.05$), and miR-26a mimics group exhibited a notably higher protein expression level of p-GSK-3β than model group ($p<0.05$). In comparison with that in sham group, the expression level of miR-26a rose markedly in both model group and miR-26a mimics group ($p<0.05$), and its expression level in miR-26a mimics group was dramatically higher than that in model group ($p<0.05$). Additionally, the TUNEL-positive cells were considerably increased in both model group and miR-26a mimics group in comparison with that in sham group ($p<0.05$), and miR-26a mimics group had markedly fewer TUNEL-positive cells than model group ($p<0.05$).

CONCLUSIONS: MiR-26a activates the GSK-3β signaling pathway to inhibit myocardial cell apoptosis after AMI.

Key Words:
Acute myocardial infarction, GSK-3β signaling pathway, MiR-26a, Apoptosis.

Introduction

With the changes in people's lifestyles and increase in their living pressure, the morbidity rate of acute myocardial infarction (AMI), a clinically critical cardiovascular disease, is increasingly higher, and presents a younger trend. According to the statistics, there are at least 500,000 new cases of AMI every year, among which middle-aged males (45-60 years old) remain the high-risk population[1,2]. The greatest harm of AMI, one killer of the life health of humans, is that it often causes death of patients. As the research on AMI continues to progress, it has been realized by researchers that long-standing ischemia and hypoxia in myocardial tissues are the major causes of myocardial infarction, and multiple pathological reactions that are further induced by myocardial tissue ischemia and hypoxia serve as the leading factors affecting the prognosis of myocardial infarction, especially cell apoptosis that has important effects on the myocardial regeneration, repair and fibrosis after myocardial infarction[3].

Corresponding Author: Shuang Lu, BM; e-mail: 346568533@qq.com

Therefore, cell apoptosis is considered as the crucial starting point for studies on AMI.

Micro ribonucleic acid (miR)-26a, as an important miRNA family member, can regulate the activation of several downstream signaling pathways and the expressions of various effector molecules to play an important regulatory role in the pathological and physiological processes, such as cell proliferation and apoptosis[4,5]. The vital glycogen synthase kinase 3 beta (GSK-3β) signaling pathway has been confirmed to be closely related to cell apoptosis. According to the findings in a study, GSK-3β can be phosphorylated under the stimulation by a variety of cytokines to activate the GSK-3β signaling pathway and further exert a pivotal anti-apoptotic effect, thereby alleviating the damage to cells, tissues, and organisms[6].

The present study, therefore, aims to observe the influence of miR-26a on myocardial cell apoptosis in rats with acute myocardial infarction *via* the GSK-3β pathway and further elucidate the role of miR-26a in AMI and its mechanism of action.

Materials and Methods

Laboratory Animals and Grouping

A total of 36 female Sprague-Dawley rats weighing (200±10) g were randomly assigned into sham group (n=12), model group (n=12), and miR-26a mimics group (n=12). They were raised in the Laboratory Animal Center and given purified water and adequate feed daily in a 12/12 h light-dark cycle, and the present study conformed to the requirements of the Laboratory Animal Ethics Committee. This study was approved by the Animal Ethics Committee of Jinzhou Medical University.

Main Reagents and Instruments

MiR-26a mimics (Boster, Wuhan, China), anti-B-cell lymphoma 2 (Bcl-2) antibody, anti-Bcl-2 associated X protein (Bax) antibody and anti-phosphorylated GSK-3β (p-GSK-3β) antibody (Abcam, Cambridge, MA, USA), immunohistochemistry and terminal deoxynucleotidyl transferase-mediated dUTP nick end labeling (TUNEL) kits (Fuzhou Maixin Biotech. Co., Ltd., Fuzhou, China), AceQ quantitative polymerase chain reaction (qPCR) SYBR Green Master Mix kit and HiScript II Q RT SuperMix for qPCR [+genomic deoxyribonucleic acid (+gDNA) wiper] kit (Vazyme Biotech, Nanjing, China), optical microscope (Leica DMI 4000B/DFC425C, Wetzlar, Germany), and fluorescence qPCR instrument (ABI 7500, Applied Biosystems, Foster City, CA, USA).

Modeling and Treatment in Each Group

The rats were intraperitoneally injected with 2.5% pentobarbital sodium at 30 mg/kg. Following successful anesthesia, the rats were fixed on an operating table, and the fur was shaved, followed by skin preparation and sterile draping. Then, they were connected to an animal electrocardiograph, and endotracheal intubation was performed between the 3rd and 4th cartilaginous rings. Subsequently, a respirator was connected, with the tidal volume and inspiratory/expiratory ratio set as 7 mL/kg and 1:1, respectively. An about 3 cm-long longitudinal incision was made around the left sternum to cut open skin, muscle, and fascia successively, and the 3rd and 4th ribs were cut off to fully expand the thoracic cavity and expose the heart. Afterwards, the pericardium was sheared open carefully using ophthalmic forceps, and a No.0 silk thread was passed through the space between the left atrial appendage and arterial cone. The electrocardiogram response in the electrocardiograph was observed, and the typical ischemic electrocardiographic pattern indicated that the model of acute myocardial infarction was prepared successfully. Finally, the incision was sutured layer by layer, while the air in the thoracic cavity was exhausted. When the rats regained consciousness, the respirator was removed, and they were kept warm and fed separately in cages.

In sham group, only the thoracic cavity of the rats was opened to expose the heart, with no No.0 silk thread passing through the space between the left atrial appendage and arterial cone, and after layer-by-layer suturing, the rats were kept with normal feed and purified water every day. After the model of AMI was successfully established by the above method, the rats in model group were fed with normal diet and purified water daily and intraperitoneally injected with normal saline once a day, while those in miR-26a mimics group were injected with miR-26a mimics using a microinjector through the anterior wall myocardium of the left ventricle, and with the thoracic cavity closed, they were given normal feed and purified water daily. At 48 h after operation, all the rats were sacrificed for sampling.

Sampling

After all the rats were anesthetized, the thoracic cavity was cut open to expose the abdominal aorta from which blood was then drawn using disposable blood lancets and stored for later use. Subsequently, 6 rats in each group were subjected to perfusion fixation with paraformaldehyde, and the cardiac tissues were taken out when the limbs of the rats were stiff, and fixed in paraformaldehyde for another 48 h. Besides, the cardiac tissues of the remaining 6 rats in each group were directly sampled into Eppendorf (EP) tubes (Hamburg, Germany) and stored in an ultra-low temperature refrigerator for later use.

Immunohistochemistry

The pre-paraffin-embedded tissues were sliced into 5 μm-thick sections, placed in warm water at 42°C for extending, mounting, and baking and prepared into paraffin-embedded tissue sections. Then, the tissue sections were soaked in xylene solution and gradient ethanol for conventional de-paraffinization and hydration, respectively. Subsequently, the resulting sections were immersed in citrate buffer and heated repeatedly in a micro-wave oven for 3 times (heating for 3 min and braising for 5 min per time) for complete antigen retrieval. After rinsing, the tissue sections were added dropwise with endogenous peroxidase blocker, reacted for 10 min, rinsed, and sealed with goat serum for 20 min. With the goat serum blocking solution discarded, the tissue sections were incubated with the anti-Bax and anti-Bcl-2 primary antibodies (1:200) in a refrigerator at 4°C overnight. On the next day, the sections were rinsed, added with the secondary antibody solution in drops, reacted for 10 min and fully washed, followed by reaction with streptomycin avidin-peroxidase solution for 10 min and color development using diaminobenzidine (DAB). Finally, cell nuclei were counterstained using hematoxylin, and the sections were sealed and observed.

Western Blotting

The cardiac tissues stored at an ultra-low temperature were added with lysis buffer, bathed on ice for 1 h, and then centrifuged at 14,000 g in a centrifuge for 10 min, followed by protein quantification using bicinchoninic acid (BCA) method (Pierce, Rockford, IL, USA). To calculate the concentration of proteins in the tissues, the absorbance of proteins was measured using a microplate reader, and the standard curve was plotted. Then, the proteins were denaturalized and isolated *via* sodium dodecyl sulphate-polyacrylamide gel electrophoresis (SDS-PAGE) that was terminated when the marker protein stayed at the bottom of the glass plate in a straight line. Subsequently, the proteins were transferred onto polyvinylidene difluoride (PVDF) membranes (Roche, Basel, Switzerland), added with sealing solution, reacted for 1.5 h, and incubated with anti-p-GSK-3β primary antibody (1:1,000) and secondary antibody (1:1,000) successively. After rinsing, images were fully developed in the dark through reaction with chemiluminescent reagent for 1 min.

QPCR

The cardiac tissues stored were added with ribonucleic acid (RNA) extraction reagent to extract the total RNA from the specimens. Then, the total RNA extracted was reversely transcribed into complementary DNA (cDNA). The reaction was performed in a system (20 μL) under the following conditions: reaction at 53°C for 5 min, pre-denaturation at 95°C for 10 min, denaturation at 95°C for 10 s, and annealing at 62°C for 30 s, for 35 cycles. After the value of ΔCt was calculated, the expression differences in the target genes were analyzed. The detailed primer sequences are shown in Table I.

TUNEL Assay

The tissues embedded in paraffin in advance were made into 5 μm-thick sections, extended, mounted, and baked in warm water at 42°C and prepared into paraffin-embedded tissue sections.

Table I. Primer sequences.

Name	Primer sequences
MiR-26a	Forward: 5'GTGGCATTACATAGTCAGCA3' Reverse: 5'GTGCAGGGTCCGAGGT3'
U6	Forward: 5'CTCGCTTCGGCAGCACATAT3' Reverse: 5'TTGCGTGTCATCCTTGCG3'

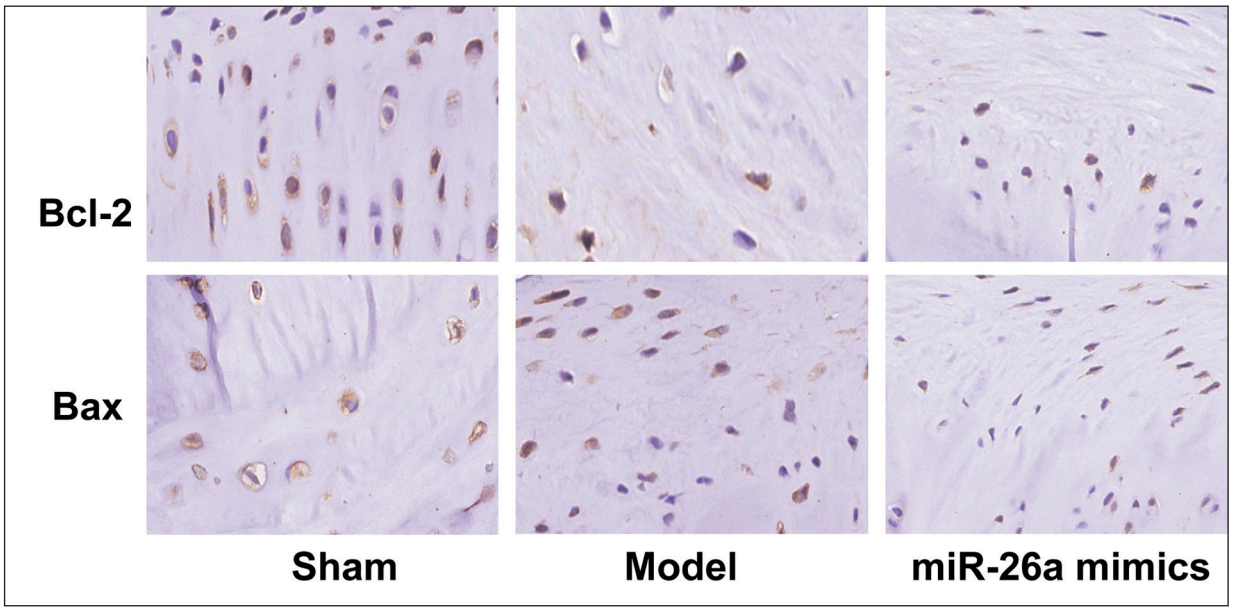

Figure 1. Expressions of Bax and Bcl-2 detected *via* immunohistochemistry (magnification ×200).

Then, these sections were routinely de-paraffinized and hydrated by immersing in xylene solution and gradient ethanol successively. Subsequently, the resulting sections were added dropwise with TdT reaction solution for reaction in the dark for 1 h and incubated with deionized water for 15 min to terminate the reaction. After the activity of endogenous peroxidase was blocked by adding hydrogen peroxide in drops, the sections were added dropwise with working solution, reacted for 1 h, rinsed, added with DAB solution in drops for color development and rinsed again. Finally, the sections were sealed and observed.

Statistical Analysis

Statistical Product and Service Solutions (SPSS) 20.0 software (IBM, Armonk, NY, USA) was employed for statistical analysis. The *t*-test, corrected *t*-test, and nonparametric test were performed for data conforming to normal distribution and homogeneity of variance, those conforming to normal distribution and heterogeneity of variance, and those dissatisfying normal distribution and homogeneity of variance, respectively. Comparison among multiple groups was done using One-way ANOVA test followed by Post-Hoc Test (Least Significant Difference). Rank sum test was used for ranked data, and Chi-square test was adopted for enumeration data. p-values < 0.05 were considered statistically significant.

Results

Expressions of Bax and Bcl-2 Detected Via Immunohistochemistry

As shown in Figure 1, sham group exhibited fewer positive expressions of Bax, but more positive expressions of Bcl-2 than both model group and miR-26a mimics group. According to the statistical results (Figure 2), compared with those in sham group, the average optical density of positively expressed Bax was increased

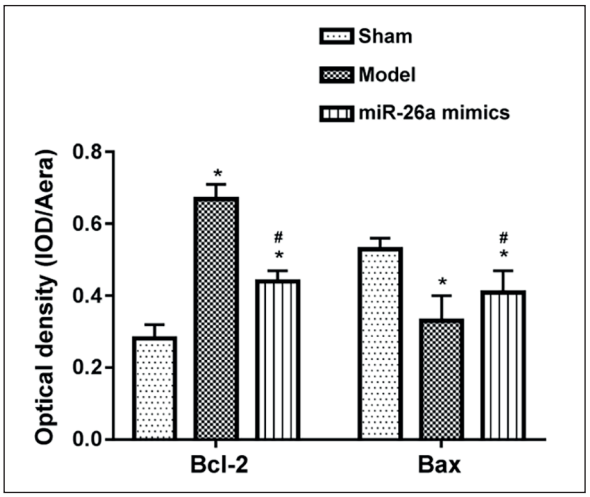

Figure 2. Optical density of positively expressed Bax and Bcl-2. Note: *p<0.05 *vs.* sham group, and $^{\#}p$<0.05 *vs.* model group.

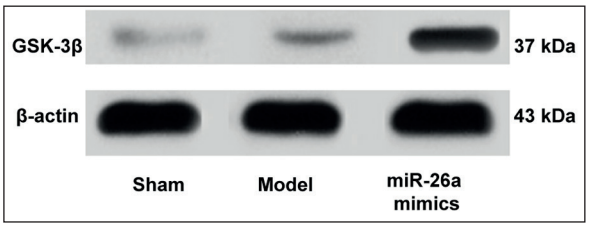

Figure 3. Protein expression detected *via* Western blotting.

substantially, but that of positively expressed Bcl-2 was notably lowered in model and miR-26a mimics groups, showing statistically significant differences (p<0.05), and miR-26a mimics group had an evidently lower average optical density of positively expressed Bax and a considerably higher average optical density of positively expressed Bcl-2 than model group, with statistically significant differences (p<0.05).

Western Blotting Results

As shown in Figure 3, sham group exhibited a lower protein expression level of GSK-3β than model group and miR-26a mimics group. The statistical results revealed that the relative protein expression level of GSK-3β was substantially elevated in model and miR-26a mimics groups compared with that in sham group, and the differences were statistically significant (p<0.05). Moreover, the relative protein expression level in miR-26a mimics group was notably higher than that in model group, showing a statistically significant difference (p<0.05; Figure 4).

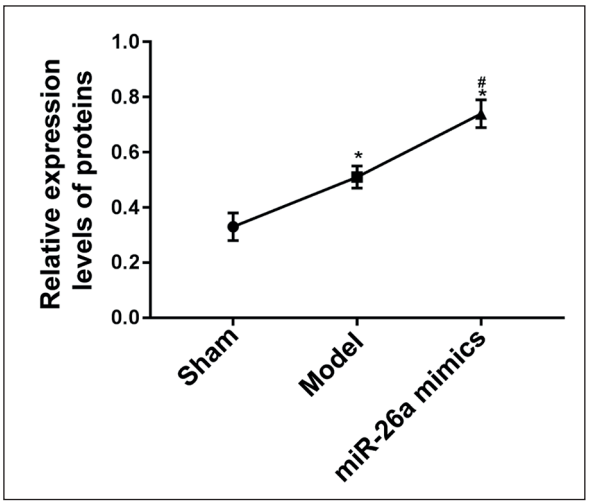

Figure 4. Relative expression levels of proteins in each group. Note: *p<0.05 *vs.* sham group, and #p<0.05 *vs.* model group.

QPCR Results

Compared with that in sham group, the relative expression level of miR-26a was markedly raised in the other two groups, with statistically significant differences (p<0.05), and its relative expression level in miR-26a mimics group was remarkably higher than that in model group, displaying a statistically significant difference (p<0.05; Figure 5).

Apoptosis Rate Measured Via TUNEL Staining

Apoptotic cells are tan and sham group had fewer such cells than the other two groups (Figure 6). As shown in Figure 7, compared with that in sham group, the average optical density of TUNEL-positive cells was substantially increased in the other two groups, showing statistically significant differences (p<0.05), and the average optical density in miR-26a mimics group was notably higher than that in model group, with a statistically significant difference (p<0.05).

Discussion

Studies have established that acute myocardial infarction is one of the leading diseases that are the most harmful to the life health of humans, and has been known as the killer of human health since it tends to cause patients' death[7,8]. AMI has very complex pathological reactions, including inflammation, oxidative stress, and apoptosis, and these

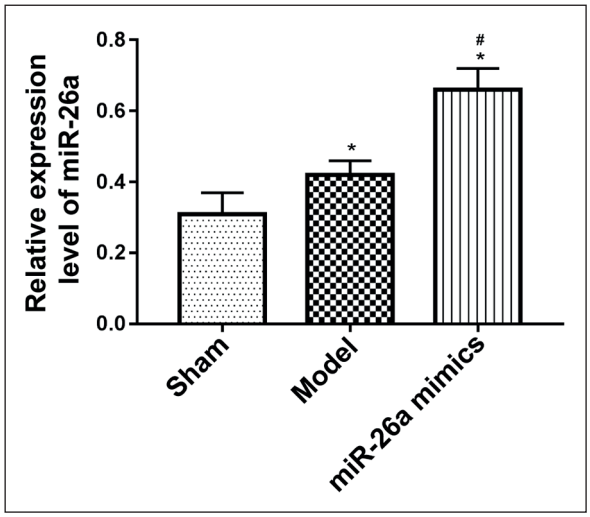

Figure 5. Relative expression level of miR-26a in each group. Note: *p<0.05 *vs.* sham group, and #p<0.05 *vs.* model group.

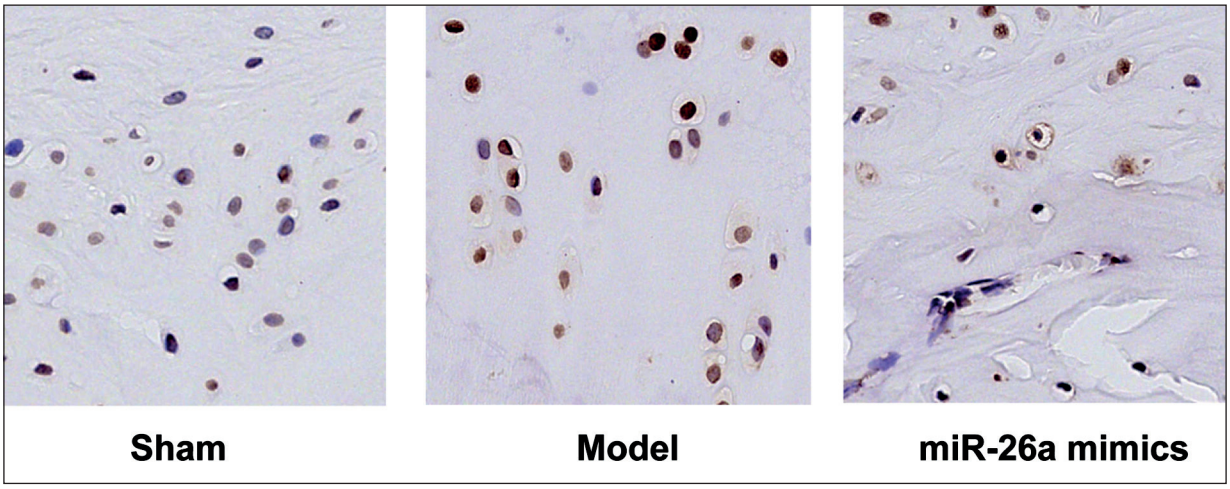

Figure 6. Cell apoptosis detected *via* TUNEL staining (magnification ×200).

complicated cellular and molecular mechanisms and a series of perplexing cascade reactions tend to affect the ventricular remodeling, playing important roles in the repair and cure after AMI[9]. In particular, apoptosis occurs in massive myocardial cells because the apoptosis-associated signaling pathways in myocardial cells are activated upon the release of various cytokines under ischemic and hypoxic conditions[10,11]. Moreover, after AMI excessive myocardial cell apoptosis can cause secondary myocardial scar hyperplasia and fibrosis[12,13] and further contribute to abnormality in tissue morphology, structural disorder, and dysfunction in myocardial infarction area, ultimately resulting in poor ventricular remodeling and patients' death in severe cases. Additionally, effectively regulating the cell apoptosis is considered of great significance for treating AMI and improving ventricular remodeling to promote the repair of myocardial cells.

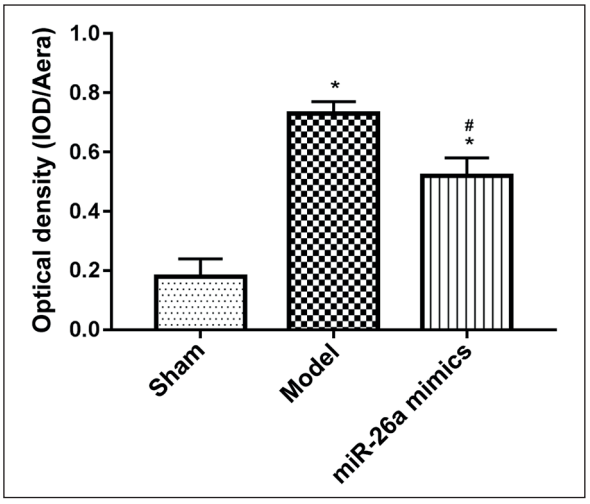

Figure 7. Average optical density of TUNEL-positive cells. Note: *$p<0.05$ *vs.* sham group, and $^{\#}p<0.05$ *vs.* model group.

The GSK-3β signaling pathway is an important signal transduction pathway that can regulate numerous physiological and pathological processes such as cell proliferation and apoptosis. The family of the crucial protein kinase B (Akt/PKB) comprises three subtypes Akt1/2/3, and once affected by various factors and cytokines in injury, Akt can be encoded by PKB gene and further activated and phosphorylated, altering spatial conformation and fully exposing two amino-acid residues for initiating phosphorylation, which ultimately exerts a pivotal signaling effect[14,15]. The active Akt can further phosphorylate GSK-3β and activate the GSK-3β signaling pathway to inhibit the downstream mPTP and prevent mitochondrial damage, thereby exerting an anti-apoptotic effect to maintain the ratio of apoptotic effector molecules Bax to Bcl-2 at a normal level[16,17].

As one of important members of the miRNA family, miR-26a has a vital regulatory effect on such physiological and pathological reactions as cell proliferation and apoptosis. Studies[18-20] have indicated that with an important anti-apoptotic effect after damage, miR-26a can effectively lower the level of cell apoptosis to play a crucial protective role in damaged tissues and cells. According to the results of this study, after AMI, Bax was abnormally highly expressed, while Bcl-2 was lowly expressed in myocardial tissues, sug-

gesting that a high level of cell apoptosis occurs in myocardial tissues. Meanwhile, the TUNEL assay also verified that myocardial cell apoptosis was aggravated, and miR-26a mimics effectively repressed the expression of Bax, but accelerated that of Bcl-2 after AMI, thereby reducing the level of myocardial cell apoptosis. Besides, the Western blotting results indicated that after AMI, the phosphorylation level of GSK-3β was raised and the GSK-3β signaling pathway was activated for the self-protection mechanism in organisms to resist apoptosis, during which miR-26a mimics further promoted the phosphorylation of GSK-3β to up-regulate the GSK-3β phosphorylation signaling pathway.

Conclusions

In summary, miR-26a inhibits myocardial cell apoptosis after acute myocardial infarction through the activation of the GSK-3β signaling pathway.

Conflict of Interest

The Authors declare that they have no conflict of interests.

References

1) Sabin P, Koshy AG, Gupta PN, Sanjai PV, Sivaprasad K, Velappan P, Vellikat Velayudhan R. Predictors of no-reflow during primary angioplasty for acute myocardial infarction, from Medical College Hospital, Trivandrum. Indian Heart J 2017; 69 Suppl 1: S34-S45.
2) Dreyer RP, Dharmarajan K, Hsieh AF, Welsh J, Qin L, Krumholz HM. Sex differences in trajectories of risk after rehospitalization for heart failure, acute myocardial infarction, or pneumonia. Circ Cardiovasc Qual Outcomes 2017; 10. pii: e003271.
3) Noguchi T, Yasuda S, Shibata T, Kawakami S, Tanaka T, Asaumi Y, Kanaya T, Nagai T, Nakao K, Fujino M, Nagatsuka K, Ishibashi-Ueda H, Nishimura K, Miyamoto Y, Kusano K, Anzai T, Goto Y, Ogawa H. Response to letter regarding article, "prevalence, clinical features, and prognosis of acute myocardial infarction attributable to coronary artery embolism". Circulation 2016; 133: e379.
4) Sahu SK, Kumar M, Chakraborty S, Banerjee SK, Kumar R, Gupta P, Jana K, Gupta UD, Ghosh Z, Kundu M, Basu J. MicroRNA 26a (miR-26a)/KLF4 and CREB-C/EBPbeta regulate innate immune signaling, the polarization of macrophages and the trafficking of Mycobacterium tuberculosis to lysosomes during infection. PLoS Pathog 2017; 13: e1006410.
5) Lu J, Song G, Tang Q, Yin J, Zou C, Zhao Z, Xie X, Xu H, Huang G, Wang J, Lee DF, Khokha R, Yang H, Shen J. MiR-26a inhibits stem cell-like phenotype and tumor growth of osteosarcoma by targeting Jagged1. Oncogene 2017; 36: 231-241.
6) McCubrey JA, Fitzgerald TL, Yang LV, Lertpiriyapong K, Steelman LS, Abrams SL, Montalto G, Cervello M, Neri LM, Cocco L, Martelli AM, Laidler P, Dulinska-Litewka J, Rakus D, Gizak A, Nicoletti F, Falzone L, Candido S, Libra M. Roles of GSK-3 and microRNAs on epithelial mesenchymal transition and cancer stem cells. Oncotarget 2017; 8: 14221-14250.
7) Phan K, Phan S, Khuong JN, Yan TD. Intra-aortic balloon pump therapy for acute myocardial infarction: trial sequential analysis. Int J Cardiol 2016; 202: 520-521.
8) Heusch G, Gersh BJ. The pathophysiology of acute myocardial infarction and strategies of protection beyond reperfusion: a continual challenge. Eur Heart J 2017; 38: 774-784.
9) O'Donoghue ML, Glaser R, Cavender MA, Aylward PE, Bonaca MP, Budaj A, Davies RY, Dellborg M, Fox KA, Gutierrez JA, Hamm C, Kiss RG, Kovar F, Kuder JF, Im KA, Lepore JJ, Lopez-Sendon JL, Ophuis TO, Parkhomenko A, Shannon JB, Spinar J, Tanguay JF, Ruda M, Steg PG, Theroux P, Wiviott SD, Laws I, Sabatine MS, Morrow DA; LATITUDE-TIMI 60 Investigators. Effect of Losmapimod on cardiovascular outcomes in patients hospitalized with acute myocardial infarction: a randomized clinical trial. JAMA 2016; 315: 1591-1599.
10) Shi ZY, Liu Y, Dong L, Zhang B, Zhao M, Liu WX, Zhang X, Yin XH. Cortistatin improves cardiac function after acute myocardial infarction in rats by suppressing myocardial apoptosis and endoplasmic reticulum stress. J Cardiovasc Pharmacol Ther 2017; 22: 83-93.
11) Li T, Wei X, Evans CF, Sanchez PG, Li S, Wu ZJ, Griffith BP. Left ventricular unloading after acute myocardial infarction reduces MMP/JNK associated apoptosis and promotes FAK cell-survival signaling. Ann Thorac Surg 2016; 102: 1919-1924.
12) Zhang Y, Li C, Meng H, Guo D, Zhang Q, Lu W, Wang Q, Wang Y, Tu P. BYD ameliorates oxidative stress-induced myocardial apoptosis in heart failure post-acute myocardial infarction via the P38 MAPK-CRYAB signaling pathway. Front Physiol 2018; 9: 505.
13) Chen H, Xu Y, Wang J, Zhao W, Ruan H. Baicalin ameliorates isoproterenol-induced acute myocardial infarction through iNOS, inflammation and oxidative stress in rat. Int J Clin Exp Pathol 2015; 8: 10139-10147.
14) Du X, Xu H, Jiang H, Xie J. Akt/Nrf2 activated upregulation of heme oxygenase-1 involves in the role of Rg1 against ferrous iron-induced neurotoxicity in SK-N-SH cells. Neurotox Res 2013; 24: 71-79.
15) Huang CS, Lin AH, Yang TC, Liu KL, Chen HW, Lii CK. Shikonin inhibits oxidized LDL-induced mono-

cyte adhesion by suppressing NFkappaB activation via up-regulation of PI3K/Akt/Nrf2-dependent antioxidation in EA.hy926 endothelial cells. Biochem Pharmacol 2015; 93: 352-361.

16) Zhang Y, Huang NQ, Yan F, Jin H, Zhou SY, Shi JS, Jin F. Diabetes mellitus and Alzheimer's disease: GSK-3beta as a potential link. Behav Brain Res 2018; 339: 57-65.

17) Xu LZ, Xu DF, Han Y, Liu LJ, Sun CY, Deng JH, Zhang RX, Yuan M, Zhang SZ, Li ZM, Xu Y, Li JS, Xie SH, Li SX, Zhang HY, Lu L. BDNF-GSK-3beta-beta-catenin pathway in the mPFC is involved in antidepressant-like effects of Morinda officinalis oligosaccharides in rats. Int J Neuropsychopharmacol 2017; 20: 83-93.

18) Zhang B, Liu XX, He JR, Zhou CX, Guo M, He M, Li MF, Chen GQ, Zhao Q. Pathologically decreased miR-26a antagonizes apoptosis and facilitates carcinogenesis by targeting MTDH and EZH2 in breast cancer. Carcinogenesis 2011; 32: 2-9.

19) Ichikawa T, Sato F, Terasawa K, Tsuchiya S, Toi M, Tsujimoto G, Shimizu K. Trastuzumab produces therapeutic actions by upregulating miR-26a and miR-30b in breast cancer cells. PLoS One 2012; 7: e31422.

20) Cui C, Xu G, Qiu J, Fan X. Up-regulation of miR-26a promotes neurite outgrowth and ameliorates apoptosis by inhibiting PTEN in bupivacaine injured mouse dorsal root ganglia. Cell Biol Int 2015; 39: 933-942.